AIR QUALITYMEASUREMENT USING REMOTE SENSING AND DIGITAL IMAGES PROCESSING TECHNIQUES

Lim, H. S., Mat Jafri, M. Z. Abdullah, K. and Ahmad A.N.
School of Physics, Universiti Sains Malaysia, 11800 Minden, Pulau Pinang

Abstract: A conventional digital camera Kodak DC 290 was used as a sensor to capture digital images of our reference targets. The digital images were separated into three bands namely red, green and blue bands for multispectral algorithm calibration. In-situ measurements of corresponding air pollution parameters were carried out at the ASMA air pollution station in Universiti Sains Malaysia campus, Penang. The selected parameter was particulate matter less than 10 micron (PM10). We put up four different colour paper (Red, Green, Blue and Black) on the wall of a building as reference surfaces. Digital images were captured at close and far distance from the colour papers/wall of the building. These in-situ measurements were then used as the dependent variables in deriving the air quality information using the digital camera data. In fact, air quality parameters can be measured using ground instrument such as air sampler. But these instruments are quite expensive, and a limited number of the air pollutant stations are available in each area. Most countries have established a network for measuring the air quality levels. Due to the high cost and limited number of the air pollutant stations in the each area, they cannot provide a good spatial distribution of the air pollutant reading over a city. The objective of this study was to test the potential of using remote sensing and digital image processing techniques for the air quality measurements. The digital numbers of the three bands were converted into irradiance and then reflectance. The relationship between the reflectance and the corresponding air quality data was determined using regression analysis. A new algorithm was developed for detecting air pollution from the digital camera images chosen based on the highest correlation coefficient, R and lowest root mean square error, RMS for PM10. The algorithm used was based on the apparent reflectance values detected at near and far distances from the refence surface, and these in turn can be related to the concentration of the air pollutants. The coefficients of the calibrated algorithm were determined and used in estimating the air pollution level. The newly developed algorithm produced a high degree of accuracy with the correlation coefficient (R) of 0.9001 and the root-mean-square error (RMS) of 5.1008 $\mu g/m^3$ for PM10. Comparison was made between the air pollution parameter and the results using different colour paper or wall of a building as a reference surface. We found that the red colour paper produced the best result when it was used as a reference surface in this study. The pollutant's concentration can be estimated accurately at a relatively much cheaper cost compared with other techniques.

Keywords: Digital camera, Air quality, Algorithm

INTRODUCTION

Air pollution causes a number of health problems and it has been linked with illnesses and deaths from heart or lung diseases. Nowadays, air quality is a major problem in many developed countries and they having build up their own network for measuring the air quality levels. Malaysia also has build up our network for monitoring our environment. A network is composed of static measuring stations, which allow continuous measurements of air pollution parameters. Data are collected hourly which include five types of the air pollution constituently such as particulate matter less than 10 micron (PM10), sulphur dioxide (SO_2), nitrogen dioxide (NO_2), carbon monoxide (CO), and ozone (O_3). This network is managed by Alam Sekitar Malaysia Sdn. Bhd. (ASMA), agency contracted by the Department of Environment Malaysia to measure air quality in the country.

Remote sensing techniques have been wide used for environmental pollution application such as water quality [2, 3, 5] and air pollution [7]. Several studies had shown the relationships between satellite data and air pollution concentration [6, 8]. But the main drawback of satellite images is the difficulty in obtaining cloud-free scenes especially at the Equatorial region. This problem can be overcome by using airborne images. In fact, air quality can be measured using ground instrument such as air samplers. But these instruments are quite expensive and a limited number of stations are available in each area. So, they cannot provide a good spatial distribution of the air pollutant readings over a city. The objective of this study is to test the potential of using remote sensing and digital image processing techniques for air

quality measurements. The digital images were captured using a normal digital camera, Kodak DC 290. We used visible digital camera imagery for this purposed. Other researchers used satellite data in such environment atmospheric studies such as NOAA-14 AVHRR [1] and TM Landsat [8]. In-situ measurements of corresponding air pollution parameters collected at the air pollution station in University Sains Malaysia, Penang, were needed for algorithm calibration. The air quality in situ data used in this study were provide by ASMA. Only one-air quality parameter was used in this study, namely PM10. Various types of algorithms were tested and the accuracies were noted.

MATERIALS AND METHODS

Study Area

The selected air quality station was located in USM campus at longitude of 100^0 17.864' and latitude of 5^0 21.528' (Figure 1). The site consists mainly of undulating land has many assets that make it an ideal University campus. University Sains Malaysia is situated in the northeast district of Penang island (Figure 1).

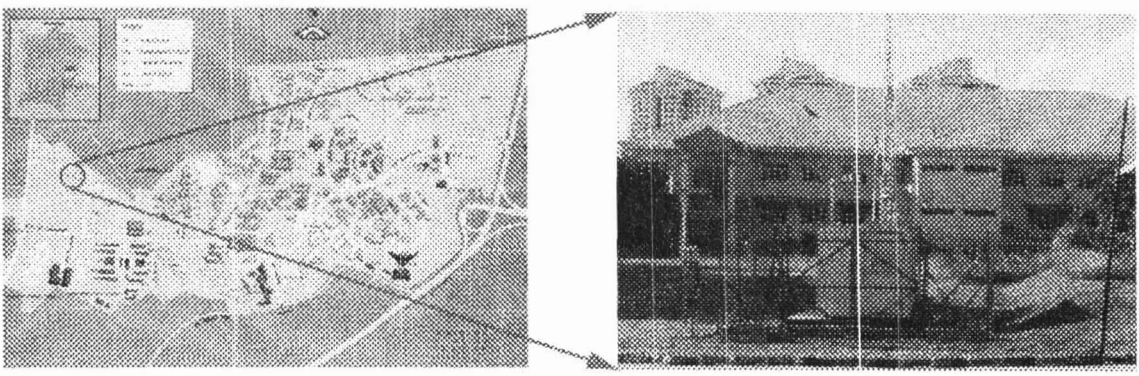

Figure 1: Study area and Air Quality Station

Methodology

The digital images were captured for a period of five days from 5-12-2003 until 9-12-2003 starting from 9.00 am. to 5.00 p.m. This air pollution station was selected in this study due to several reasons, a) It is in the USM campus, so it is easy to capture the digital images hourly. b) The presence of a construction site near the station, so we expected that the PM10 level to be high during working time. c) The USM bus stop was near to the station, so we expected that the CO levels to be high during busy times in the morning and evening. d) A building near the station can be used to stick up the colour paper on its wall for reference surface. The air quality station belongs to ASMA is shown in Figure 1. The digital images were captured hourly because the air quality data were also collected hourly by ASMA through the network.

We used colour paper and the wall of the building as our reference targets. At first, we put four-coloured paper on the wall of a building before we captured the images as our reference surface. We will capture the digital images horizontally and these are 90^0 with the colour paper. We captured the digital images of the reference targets by using the digital camera at near and far distance from the targets. The far distance between the building and the camera was 100 meter. Presumption made in this study was that the air quality measurement represents a column of 100 x 5 x 5 m^3 around the air pollution stations.

RESULTS AND DISCUSSIONS

All image-processing tasks were carried out using PCI EASI/PACE version 6.2 digital image processing software at the School Of Physics, University Sains Malaysia (USM). The digital images were separated into three bands (red, green and blue). The average DN for each digital image captured at near and far distance from the reference targets were extracted.

All the DN values were converted into irradiance using equation 1, 2 and 3.The DNs were converted into irradiance using the digital camera coefficient calibrated for each band [4]. And then the irradiances were converted to reflectance using the equation 4 for each band. The solar angles and Earth-Sun distance were calculated corresponding to the time the digital image acquisition. Mean solar exoatmospheric irradiances used in this study were 1555 $W/m^2/\mu m$, 1843 $W/m^2/\mu m$ and 1970 $W/m^2/\mu m$ for red, green and blue bands respectively.

The calibrated digital camera coefficients are

$$y_1 = 0.0005x_1 + 0.0738 \quad (1)$$
$$y_2 = 0.0007x_2 + 0.0517 \quad (2)$$
$$y_3 = 0.0006x_3 + 0.0497 \quad (3)$$

where
y_1 = irradiance for red band (Wm^{-2} nm^{-1})
y_2 = irradiance for green band (Wm^{-2} nm^{-1})
y_3 = irradiance for blue band (Wm^{-2} nm^{-1})
x_1 = digital number for red band
x_2 = digital number for green band
x_3 = digital number for blue band

The reflectance is given by

$$R = \frac{\pi L(\lambda) d^2}{E(\lambda)\cos\theta} \quad (4)$$

where
L (λ)= Radiance (Wm^{-2} sr^{-1} μm^{-1})
d = Earth-Sun distance in astronomical units
= {1.0-0.016729cos[0.9856(D-4)]} where (D = day of the year)
E (λ) = Mean solar exoatmospheric irradiance (Wm^{-2} μm^{-1})
= Solar zenith angle (degrees)

The relationship between the reflectance and the corresponding air quality data for the pollutant was carried out using regression analysis. Different forms of algorithm were tested with the data set. For each regression model the correlation coefficient, R, and the root-mean-square deviation, RMS, were noted. The best model was chosen based on the highest correlation coefficient, R^2 and lowest root mean square error, RMS for PM10. The proposed algorithm produced the highest correlation coefficient between the predicted and the measured TSS values and lowest RMS value compared to the other algorithms. With the present data set, the R and RMS values produced by the proposed algorithm for PM 10 using four different colour paper as a refence target are show in the table 1, 2, 3 and 4.

Table 1: Regression results using different forms of algorithms for air pollutant (Red colour paper as a reference target)

Algorithm	R	RMS ($\mu g/m^3$)
PM 10=$a_0+a_1(x_1-x_2)+a_2(x_3-x_4)+a_3(x_5-x_6)+a_4(x_1-x_2)^2+a_5(x_3-x_4)^2+a_6(x_5-x_6)^2$	0.8243	5.8162
PM 10= $a_0+a_1x_1- a_2x_2+ a_3x_3- a_4x_4+ a_5x_5- a_6x_6++ a_7x_1^2- a_8x_2^2+ a_9x_3^2- a_{10}x_4^2+ a_{11}x_5^2- a_{12}x_6^2$	0.8907	5.1929
PM 10= $a_0+ a_1 (x_1+x_2)+ a_2(x_3+x_4)+ a_3(x_5+x_6)+ a_4(x_1+x_2)^2+ a_5(x_3+x_4)^2+ a_6(x_5+x_6)^2$	0.7133	7.1952
PM 10= $a_0+ a_1 (x_1/x_2)+ a_2 (x_3/x_4)+ a_3 (x_5/x_6)+ a_4(x_1/x_2)^2+ a_5 (x_3/x_4)^2+ a_6(x_5/x_6)^2$	0.5233	8.7480
PM 10= a0+a*(x2/x1)+ a2(x4/x3)+ a3(x6/x5)+ a4(x2/x1)^2+ a5 (x4/x3)^2+ a6(x6/x5)^2	0.5630	8.4844
PM 10= $a_0+ a_1x_1+ a_2x_2+ a_3x_3+ a_4x_4+ a_5x_5+ a_6x_6+ a_7x_1^2+ a_8x_2^2+ a_9x_3^2+ a_{10}x_4^2+ a_{11}x_5^2+ a_{12}x_6^2$	0.8907	5.1929
PM 10= $a_0+ a_1\ln(x_1+x_2)+ a_2\ln(x_3+x_4)+ a_3\ln(x_5+x_6)+ a_4(\ln(x_1+x_2)\_^2+ a_5(\ln(x_3+x_4))^2+ a_6 (\ln(x_5+x_6))^2$	0.6971	7.3605
PM 10= $a_0+ a_1\ln(x_1/x_2)+ a_2\ln(x_3/x_4)+ a_3\ln(x_5/x_6)+ a_4(\ln(x_1/x_2))^2+ a_5(\ln(x_3/x_4))^2+ a_6(\ln(x_5/x_6))^2$	0.5456	8.6035
PM 10= $a_0+ a_1\ln(x_1)+ a_2\ln(x_2)+ a_3\ln(x_3)+ a_4\ln(x_4)+ a_5\ln(x_5)+ a_6\ln(x_6)+$ a7(ln(x1))^2+ $a_8(\ln(x_2))^2+ a_9(\ln(x_3))^2+ a_{10}(\ln(x_4))^2+ a_{11}(\ln(x_5))^2+ a_{12}(\ln(x_6))^2$	0.9001	5.1008

* x_1, x_2, x_3, x_4, x_5 and x_6 are the reflectance for red (near), red (far), green (near), green (far), blue (near) and blue (far) band respectively

Table 2: Regression results using different forms of algorithms for air pollutant (Green colour paper as a reference target)

Algorithm	R	RMS ($\mu g/m^3$)
PM 10=$a_0+a_1(x_1-x_2)+a_2(x_3-x_4)+a_3(x_5-x_6)+a_4(x_1-x_2)^2+a_5(x_3-x_4)^2+a_6(x_5-x_6)^2$	0.4714	9.0539
PM 10= $a_0+a_1x_1- a_2x_2+ a_3x_3- a_4x_4+ a_5x_5- a_6x_6++ a_7x_1^2- a_8x_2^2+ a_9x_3^2- a_{10}x_4^2+ a_{11}x_5^2- a_{12}x_6^2$	0.8704	5.6239
PM 10= $a_0+ a_1 (x_1+x_2)+ a_2(x_3+x_4)+ a_3(x_5+x_6)+ a_4(x_1+x_2)^2+ a_5(x_3+x_4)^2+ a_6(x_5+x_6)^2$	0.7614	6.6549
PM 10= $a_0+ a_1 (x_1/x_2)+ a_2 (x_3/x_4)+ a_3 (x_5/x_6)+ a_4(x_1/x_2)^2+ a_5 (x_3/x_4)^2+ a_6(x_5/x_6)^2$	0.5182	8.7800
PM 10= a0+a*(x2/x1)+ a2(x4/x3)+ a3(x6/x5)+ a4(x2/x1)^2+ a5 (x4/x3)^2+ a6(x6/x5)^2	0.4969	8.9087
PM 10= $a_0+ a_1x_1+ a_2x_2+ a_3x_3+ a_4x_4+ a_5x_5+ a_6x_6+ a_7x_1^2+ a_8x_2^2+ a_9x_3^2+ a_{10}x_4^2+ a_{11}x_5^2+ a_{12}x_6^2$	0.8704	5.6239
PM 10= $a_0+ a_1\ln(x_1+x_2)+ a_2\ln(x_3+x_4)+ a_3\ln(x_5+x_6)+ a_4(\ln(x_1+x_2)\_^2+ a_5(\ln(x_3+x_4))^2+ a_6 (\ln(x_5+x_6))^2$	0.7469	6.8261
PM 10= $a_0+ a_1\ln(x_1/x_2)+ a_2\ln(x_3/x_4)+ a_3\ln(x_5/x_6)+ a_4(\ln(x_1/x_2))^2+ a_5(\ln(x_3/x_4))^2+ a_6(\ln(x_5/x_6))^2$	0.5036	8.8691
PM 10= $a_0+ a_1\ln(x_1)+ a_2\ln(x_2)+ a_3\ln(x_3)+ a_4\ln(x_4)+ a_5\ln(x_5)+ a_6\ln(x_6)+$ a7(ln(x1))^2+ $a_8(\ln(x_2))^2+ a_9(\ln(x_3))^2+ a_{10}(\ln(x_4))^2+ a_{11}(\ln(x_5))^2+ a_{12}(\ln(x_6))^2$	0.8720	5.7287

* x_1, x_2, x_3, x_4, x_5 and x_6 are the reflectance for red (near), red (far), green (near), green (far), blue (near) and blue (far) band respectively

Table 3: Regression results using different forms of algorithms for air pollutant (Blue colour paper as a reference target)

Algorithm	R	RMS ($\mu g/m^3$)
PM 10=$a_0+a_1(x_1-x_2)+a_2(x_3-x_4)+a_3(x_5-x_6)+a_4(x_1-x_2)^2+a_5(x_3-x_4)^2+a_6(x_5-x_6)^2$	0.4616	9.1071
PM 10= $a_0+a_1x_1- a_2x_2+ a_3x_3- a_4x_4+ a_5x_5- a_6x_6++ a_7x_1^2- a_8x_2^2+ a_9x_3^2- a_{10}x_4^2+ a_{11}x_5^2- a_{12}x_6^2$	0.8373	6.2456
PM 10= $a_0+ a_1 (x_1+x_2)+ a_2(x_3+x_4)+ a_3(x_5+x_6)+ a_4(x_1+x_2)^2+ a_5(x_3+x_4)^2+ a_6(x_5+x_6)^2$	0.6355	7.9266
PM 10= $a_0+ a_1 (x_1/x_2)+ a_2 (x_3/x_4)+ a_3 (x_5/x_6)+ a_4(x_1/x_2)^2+ a_5 (x_3/x_4)^2+ a_6(x_5/x_6)^2$	0.4854	8.9754
PM 10= $a_0+a*(x2/x1)+ a_2(x4/x3)+ a_3(x6/x5)+ a_4(x2/x1)\text{^}2+ a_5 (x4/x3)\text{^}2+ a_6(x6/x5)\text{^}2$	0.4843	8.9817
PM 10= $a_0+ a_1x_1+ a_2x_2+ a_3x_3+ a_4x_4+ a_5x_5+ a_6x_6+ a_7x_1^2+ a_8x_2^2+ a_9x_3^2+ a_{10}x_4^2+ a_{11}x_5^2+ a_{12}x_6^2$	0.8373	6.2456
PM 10= $a_0+ a_1\ln(x_1+x_2)+ a_2\ln(x_3+x_4)+ a_3\ln(x_5+x_6)+ a_4(\ln(x_1+x_2)\_^2+ a_5(\ln(x_3+x_4))^2+ a_6 (\ln(x_5+x_6))^2$	0.6323	7.9533
PM 10= $a_0+ a_1\ln(x_1/x_2)+ a_2\ln(x_3/x_4)+ a_3\ln(x_5/x_6)+ a_4(\ln(x_1/x_2))^2+ a_5(\ln(x_3/x_4))^2+ a_6(\ln(x_5/x_6))^2$	0.4768	9.0239
PM 10= $a_0+ a_1\ln(x_1)+ a_2\ln(x_2)+ a_3\ln(x_3)+ a_4\ln(x_4)+ a_5\ln(x_5)+ a_6\ln(x_6)+ a_7(\ln(x_1))\text{^}2+ a_8(\ln(x_2))^2+ a_9(\ln(x_3))^2+ a_{10}(\ln(x_4))^2+ a_{11}(\ln(x_5))^2+ a_{12}(\ln(x_6))^2$	0.8321	6.4920

* x_1, x_2, x_3, x_4, x_5 and x_6 are the reflectance for red (near), red (far), green (near), green (far), blue (near) and blue (far) band respectively

Table 4: Regression results using different forms of algorithms for air pollutant (Black colour paper as a reference target)

Algorithm	R	RMS ($\mu g/m^3$)
PM 10=$a_0+a_1(x_1-x_2)+a_2(x_3-x_4)+a_3(x_5-x_6)+a_4(x_1-x_2)^2+a_5(x_3-x_4)^2+a_6(x_5-x_6)^2$	0.3467	9.6295
PM 10= $a_0+a_1x_1- a_2x_2+ a_3x_3- a_4x_4+ a_5x_5- a_6x_6++ a_7x_1^2- a_8x_2^2+ a_9x_3^2- a_{10}x_4^2+ a_{11}x_5^2- a_{12}x_6^2$	0.6854	8.3181
PM 10= $a_0+ a_1 (x_1+x_2)+ a_2(x_3+x_4)+ a_3(x_5+x_6)+ a_4(x_1+x_2)^2+ a_5(x_3+x_4)^2+ a_6(x_5+x_6)^2$	0.7076	7.2546
PM 10= $a_0+ a_1 (x_1/x_2)+ a_2 (x_3/x_4)+ a_3 (x_5/x_6)+ a_4(x_1/x_2)^2+ a_5 (x_3/x_4)^2+ a_6(x_5/x_6)^2$	0.3338	9.6772
PM 10= $a_0+a*(x2/x1)+ a_2(x4/x3)+ a_3(x6/x5)+ a_4(x2/x1)\text{^}2+ a_5 (x4/x3)\text{^}2+ a_6(x6/x5)\text{^}2$	0.3457	9.6331
PM 10= $a_0+ a_1x_1+ a_2x_2+ a_3x_3+ a_4x_4+ a_5x_5+ a_6x_6+ a_7x_1^2+ a_8x_2^2+ a_9x_3^2+ a_{10}x_4^2+ a_{11}x_5^2+ a_{12}x_6^2$	0.6854	8.3181
PM 10= $a_0+ a_1\ln(x_1+x_2)+ a_2\ln(x_3+x_4)+ a_3\ln(x_5+x_6)+ a_4(\ln(x_1+x_2)\_^2+ a_5(\ln(x_3+x_4))^2+ a_6 (\ln(x_5+x_6))^2$	0.6425	7.8668
PM 10= $a_0+ a_1\ln(x_1/x_2)+ a_2\ln(x_3/x_4)+ a_3\ln(x_5/x_6)+ a_4(\ln(x_1/x_2))^2+ a_5(\ln(x_3/x_4))^2+ a_6(\ln(x_5/x_6))^2$	0.3387	9.6591
PM 10= $a_0+ a_1\ln(x_1)+ a_2\ln(x_2)+ a_3\ln(x_3)+ a_4\ln(x_4)+ a_5\ln(x_5)+ a_6\ln(x_6)+ a_7(\ln(x_1))\text{^}2+ a_8(\ln(x_2))^2+ a_9(\ln(x_3))^2+ a_{10}(\ln(x_4))^2+ a_{11}(\ln(x_5))^2+ a_{12}(\ln(x_6))^2$	0.6885	8.4889

* x_1, x_2, x_3, x_4, x_5 and x_6 are the reflectance for red (near), red (far), green (near), green (far), blue (near) and blue (far) band respectively

CONCLUSION

Preliminary, the analysis indicated that digital camera imagery could provide useful remotely sensed data for air pollutant measurements using a multiband algorithm. In this study, digital camera imageries have been introduced for air quality estimation when produced a satisfying regression algorithm result. We found that the red colour paper was the best reference surface used in this study because it produced the highest accuracy compared to the results using green, blue and black colour papers. This proposed technique give an alternative way to provide low cost digital imageries for environment atmospheric pollution application. Further study must be carried out to increase digital camera capacity to estimates air quality.

ACKNOWLEDGEMENTS

This project was carried out using the Malaysia Government IRPA grant no.08-02-05-6011 and USM short term grant FPP2001/130. We would like to thank the technical staff who participated in this project. Thanks are extended to USM for support and encouragement.

REFERENCES

1. Asmala, A. and Mazlan, H. 2002. Determination of haze using NOAA-14 AVHRR satellite data, Available online: http://www.gisdevelopment.net/aars/acrs/2002/czm/050.pdf

2. Dekker, A. G., Vos, R. J. and Peters, S. W. M. 2002. Analytical algorithms for lakes water TSM estimation for retrospective analyses of TM dan SPOT sensor data. *International Journal of Remote Sensing*. 23(1): 15–35

3. Doxaran, D., Froidefond, J. M., Lavender, S. and Castaing, P. 2002. *Spectral signature of highly turbid waters application with SPOT data to quantify suspended particulate matter concentrations.* Remote Sensing of Environment. 81: 149–161

4. Lim, H. S. 2003. Total Suspended Solids Mapping Using Digital Camera Imagery Taken From Light Aircraft. M. Sc. Theses, Unpublished.

5. Tassan, S. 1997. A numerical model for the detection of sediment concentration in stratified river plumes using Thematic Mapper data. *International Journal of Remote Sensing*. 18(12): 2699–2705

6. Ung, A., Weber, C., Perron, G., Hirsch, J., Kleinpeter, J., Wald, L. and Ranchin, T. 2001a. Air Pollution Mapping Over A City – Virtual Stations And Morphological Indicators. Proceedings of 10th International Symposium "Transport and Air Pollution" September 17 - 19, 2001 – Boulder, Colorado USA.
http://wwwcenerg.cma.fr/Public/themes_de_recherche/teledetection/title_tele_air/title_tele_air_pub/air_pollution_mappin4043.

7. Ung, A., Wald, L., Ranchin, T., Weber, C., Hirsch, J., Perron, G. and Kleinpeter, J., 2001b. Satellite data for Air Pollution Mapping Over A City- Virtual Stations, Proceeding of the 21th EARSeL Symposium, Observing Our Environment From Space: New Solutions For A New Millenium, Paris, France.Gerard Begni Editor, A., A., Balkema, Lisse, Abingdon, Exton (PA), Tokyo, pp. 147 – 151
http://www.cenerg.cma.fr/Public/themes_de_recherché/teledetection/title_tele_air/title_tele_air_pub/satellite_data_for_t.

8. Weber, C., Hirsch, J., Perron, G., Kleinpeter, J., Ranchin, T., Ung, A. and Wald, L. 2001. Urban Morphology, Remote Sensing and Pollutants Distribution: An Application To The City of Strasbourg, France. International Union of Air Pollution Prevention and Environmental Protection Associations (IUAPPA) Symposium and Korean Society for Atmospheric Environment (KOSAE) Symposium, 12th World Clean Air & Environment Congress, Greening the New Millennium. http://wwwcenerg.cma.fr/Public/themes_de_recherche/teledetection/title_tele_air/title_tele_air_pub/paper_urban_morpho.